Available online at www.sciencedirect.com
ScienceDirect
Ceramics International 38S (2012) S547–S550
CERAMICS INTERNATIONAL
www.elsevier.com/locate/ceramint

Thermal properties of $CaMgSi_2O_6$ glass–ceramics with Al_2O_3

Eung Soo Kim *, Won Jae Yeo

Department of Materials Engineering, Kyonggi University, Suwon 443-760, Republic of Korea

Available online 26 May 2011

Abstract

The thermal properties of $CaMgSi_2O_6$ glass–ceramics with Al_2O_3 were investigated as a function of Al_2O_3 content. With increasing of Al_2O_3 content, the thermal conductivity of the sintered specimen was increased up to 4 vol.% and then decreased, while the coefficient of thermal expansion (*CTE*) was decreased up to 8 vol.% and then increased. These results could be attributed to the crystallite size and rigidity of glass network, respectively. Typically, the thermal conductivity of 3.07 W/m °C and/or the *CTE* of 8.76 ppm/ °C (25–600 °C) was obtained for the specimens of $CaMgSi_2O_6$ with 4 vol.% and/or 8 vol.% of Al_2O_3 sintered at 900 °C for 3 h, respectively.
© 2011 Elsevier Ltd and Techna Group S.r.l. All rights reserved.

Keywords: C. Thermal conductivity; D. Glass ceramics; C. Coefficient of thermal expansion; $CaMgSi_2O_6$

1. Introduction

Diopside ($CaMgSi_2O_6$) has high mechanical properties (bending strength of 300 Mpa, Mohs hardness of 5–6) and good chemical resistivity. Moreover, the diopside easily tends to be glass from the processes of melting and quenching. The glass–ceramics of $CaMgSi_2O_6$ can be sintered at low temperature which is available to the temperature of co-fired with good electrodes such as silver (960 °C) and copper (1050 °C) [1].

For the multilayer packages applicable to the high-power LED, the difference of coefficient of thermal expansion (*CTE*) between chip and packages leads to solder-crack, and the heat generated by LED chips with high power tend to reduce durability and reliability of LED. Therefore, the materials with low *CTE* and high thermal conductivity should be investigated to prevent mismatch of *CTE* and to dissipate heat effectively.

Polycrystalline of glass–ceramics could be obtained by the crystallization of high viscous glass with appropriate compositions. In general, the *CTE* of glass–ceramics depends on the composition, degree of crystallization and rigidity of the glass network [2]. Also, the thermal conductivity of glass–ceramics depends on the composition, structure, intrinsic thermal conductivities, interfacial thermal resistance, particle size and shape [3].

In our previous work, *CTE* of $CaMgSi_2O_6$ glass–ceramics was increased with the degree of crystallization because the diopside shows large difference of *CTE* between amorphous phase (6.65 ppm/ °C) and crystalline phase (9.26 ppm/ °C) [2]. Also, the thermal conductivity of $CaMgSi_2O_6$ glass–ceramics was improved with increasing of the degree of crystallization. Therefore, the degree of crystallization should be controlled to improve the *CTE* and thermal conductivity of $CaMgSi_2O_6$ glass–ceramics, simultaneously for the practical applications.

Alumina (Al_2O_3) has been widely used due to the low *CTE* and high thermal conductivity as well as high hardness and good chemical inertness [1,4]. Therefore, it could be expected the *CTE* and thermal conductivity of $CaMgSi_2O_6$ glass–ceramics could be improved by the addition of Al_2O_3.

In this study, the dependence of thermal properties on the crystallization behaviors of $CaMgSi_2O_6$ glass–ceramics with Al_2O_3 was investigated as a function of Al_2O_3 content. The crystallization behaviors of glass–ceramics were also discussed based on degree of crystallization, rigidity of glass network and crystallite size.

2. Experimental procedures

High-purity (≥99.9%) oxide powders of $CaCO_3$, $MgCO_3$ and SiO_2 were used as starting materials. Mixture of powders was weighed according to the desired composition of $CaMgSi_2O_6$ and ground with ZrO_2 balls for 24 h in ethanol. The mixed powders were first melting in a platinum crucible at

* Corresponding author. Tel.: +82 31 249 9764; fax: +82 31 244 6300.
E-mail address: eskim@kyonggi.ac.kr (E.S. Kim).

0272-8842/$36.00 © 2011 Elsevier Ltd and Techna Group S.r.l. All rights reserved.
doi:10.1016/j.ceramint.2011.05.074

1500 °C for 3 h and quenched into distilled water. Then the cullet was pulverized and melted again at 1500 °C for 3 h to improve the homogeneity. Pure diopside glass frits were prepared after quenching and grinding. These glass frits were re-milled for 24 h and then mixed with Al_2O_3 (2–10 vol.%) by ball-milling for 24 h. The mixture of powder pressed into pellets isostatically under the pressure of 1500 kg/cm^2. These pellets were sintered from 850 °C to 950 °C for 3 h after holding at 745 °C for 3 h in air.

The densities of the sintered specimens were measured by Archimedes method. The differential thermal analysis (DTA) curve was obtained by a simultaneous thermal analyzer-mass spectrometer (STA 409PC – QMS 403C, NETZCH, Germany). Powder X-ray diffraction analysis (XRD, D/Max-2500V/PC, RIGAKU, Japan) and scanning electron microscope (SEM, JSM-6700F, JEOL, Japan) were used to evaluate the phases, microstructures and crystallization behavior of glass. Fourier Transform Infrared Spectroscopy (430FT-IR, JASCO, USA) was used to identify the glass network structure. The thermal conductivity and thermal expansion coefficient (25–600 °C) of the sintered specimens were obtained by a laser flash apparatus (LFA 457, NETZCH, Germany) and dilatometer (DIL 402C, NETZCH, Germany), respectively.

3. Results and discussion

Fig. 1 shows the DTA curves of $CaMgSi_2O_6$ glass with Al_2O_3 at heating rate of 5 °C/min. The strong exothermic reaction peaked from 883 °C to 887 °C is attributed to the crystallization of glass. With increasing of Al_2O_3 content, glass transition temperature (T_g), onset temperature of crystallization (T_c) and the peak temperature of crystallization (T_p) of glass powders were shifted to higher temperature. The difference of T_c from T_g (glass stability) was not changed remarkably, while the difference of T_p from T_c (crystallization rate) was decreased with Al_2O_3 content [5]. Therefore, the addition of Al_2O_3 affected the crystallization rate rather than glass stability of diopside glass.

From the results of DTA data, the sintering temperature was determined from 850 °C to 950 °C after holding at 745 °C for 3 h because the nucleation of glasses is generated at higher temperature than T_g and crystallization of glass is corresponded to a strong exothermic reaction peak of DTA curve [6]. With increasing of sintering temperature from 850 °C to 950 °C, the relative density of the specimens was increased up to 900 °C and then showed a constant value. To reduce the effects of density on the thermal properties, the optimal sintering temperature was 900 °C for highest relative density. However, the relative density of the specimens sintered from 850 °C to 950 °C for 3 h was decreased with Al_2O_3 content.

Fig. 2 shows the XRD patterns of $CaMgSi_2O_6$ with Al_2O_3 specimens sintered from 850 °C to 950 °C for 3 h. Monoclinic diopside ($CaMgSi_2O_6$) phase and rhombohedral α-Al_2O_3 phase was detected for the specimens with 2 vol.% Al_2O_3 sintered from 850 °C to 950 °C for 3 h (Fig. 2(a)). The XRD patterns of sintered specimens were not changed remarkably with sintering temperature from 850 °C to 950 °C. However, the secondary phase of α-Al_2O_3 was increased with Al_2O_3 content for the specimens sintered at 900 °C for 3 h (Fig. 2(b)). Based on the XRD patterns of the specimens, the reaction compounds between the $CaMgSi_2O_6$ and Al_2O_3 were not detected, which in turn, the chemical reactions between the $CaMgSi_2O_6$ and Al_2O_3 were not confirmed.

Since the thermal properties of glass–ceramics depend on the degree of crystallization and crystallite size, those factors should be considered. Due to the large difference of *CTE* between amorphous phase and crystalline phase of diopside, *CTE* is strongly dependent on the degree of crystallization, which was calculated by Challa–Hermans–Weidinger equation [2,7].

$$X_c\,(\%) = \left\{1 - \left(\frac{1}{(I_\alpha)_{2\theta*}}\right)(I_\alpha)_{2\theta}\right\} \times 100 \quad (1)$$

where $(I_\alpha)_{2\theta*}$ and $(I_\alpha)_\theta$ are the intensity of the glass powders and sintered specimens at same range of 2θ, respectively. With increasing of Al_2O_3 content, the degree of crystallization was

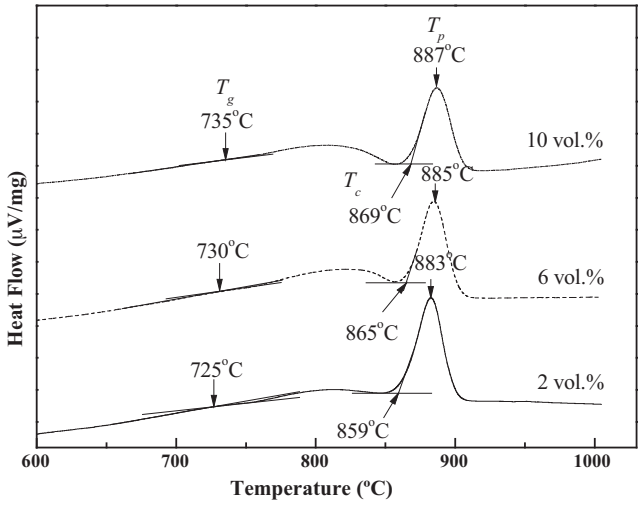

Fig. 1. DTA curve of $CaMgSi_2O_6$ glass with Al_2O_3 at heating rate of 5 °C/min.

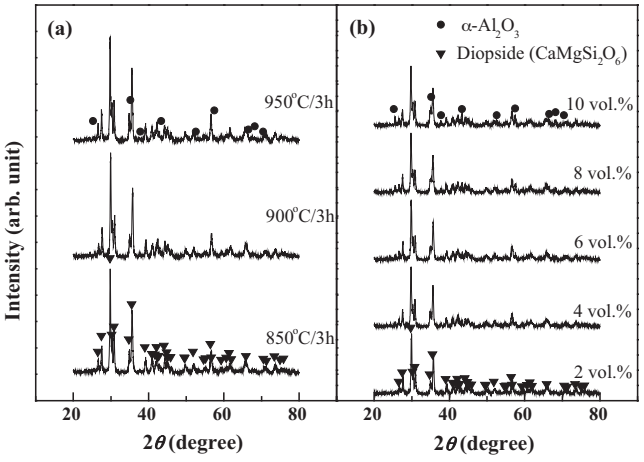

Fig. 2. XRD patterns of $CaMgSi_2O_6$ with (a) 2 vol.% of Al_2O_3 specimens sintered from 850 °C to 950 °C for 3 h and (b) 2-10 vol.% of Al_2O_3 specimens sintered at 900 °C for 3 h.

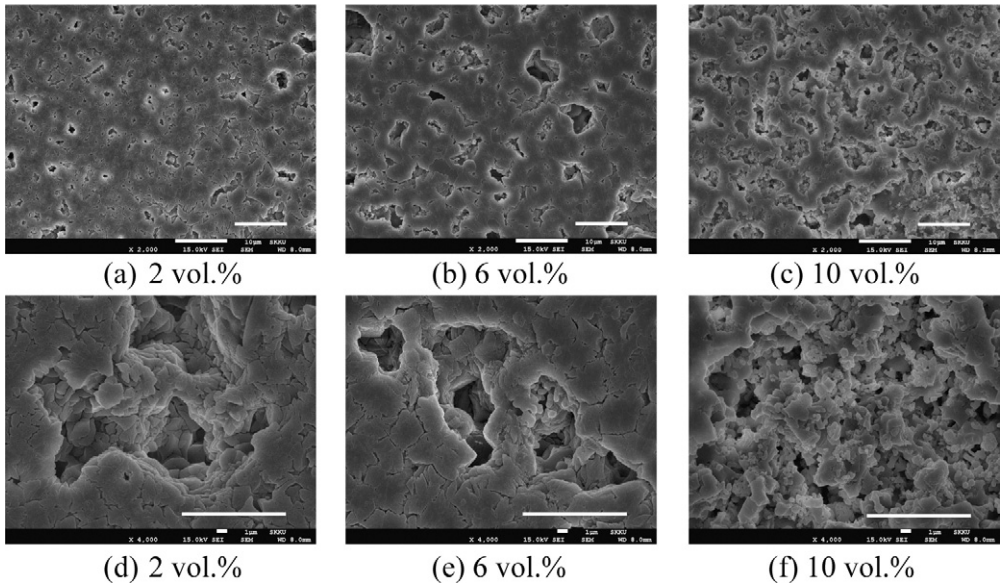

Fig. 3. SEM micrographs of $CaMgSi_2O_6$ with Al_2O_3 specimens sintered at 900 °C for 3 h (bar = 10 μm).

decreased from 84% to 78%. Also, the thermal conductivity is dependent on crystallite size due to the amount of interfaces [8]. The average crystallite size of specimens can be estimated by Scherrer equation [9].

$$D = \frac{0.89\lambda}{\beta \cos\theta} \quad (2)$$

where D is the average crystallite size, λ is the wavelength of the CuK_α-radiation, β is the corrected full width at half-maximum, and θ is the Bragg angle. The average crystallite size of the sintered specimens was decreased from 40.5 nm to 33.9 nm with increasing of Al_2O_3 content.

SEM micrographs of $CaMgSi_2O_6$ with Al_2O_3 specimens sintered at 900 °C for 3 h are shown in Fig. 3. The porosity was increased with Al_2O_3 content, which is agreed with the relative density of the specimens. Furthermore, the small gains were appeared from inside of the sintered specimen above 6 vol.% Al_2O_3. The numbers of small grains were increased with Al_2O_3 content. These results could be attributed to the reduction of average crystallite size with Al_2O_3 content as calculated from XRD patterns of the specimens.

Moreover, thermal properties of glass–ceramics are dependent on amorphous phase as well as crystalline phases. Generally, *CTE* of glasses is dependent on the asymmetry of the amplitude of thermal vibrations, which decreases with the increase of rigidity of the glass network. Modifying cations decrease the rigidity of the glass network by introducing non-bridging oxygen ions and therefore increase the *CTE* of the glass [2]. The rigidity of glass network can be estimated by FTIR.

FTIR spectra of $CaMgSi_2O_6$ with Al_2O_3 specimens sintered at 900 °C for 3 h are shown in Fig. 4. The bands in the region of 400–1200 cm^{-1} for diopside were confirmed to be in accordance with the report of Omori [10]. The three broad transmittance bands in the region of 400–600 cm^{-1}, 600–800 cm^{-1} and 800–1200 cm^{-1} were defined as the bending vibrations of non-bridging oxygen atoms (O–Mg–O), non-bridging oxygen atoms (O–Si–O) and bridging oxygen atoms (Si–O), respectively. The peak at 605 cm^{-1} was observed which could be related to the Al–O vibration [11]. However, the spectrum in the region of 420–500 cm^{-1} of $CaMgSi_2O_6$ with 10 vol.% of Al_2O_3 was shifted to low wavenumber which was attributed to the non-bridging oxygen atoms (O–Mg–O) of chain deformation due to the decrease of the rigidity of glass network [2].

Fig. 5 shows the dependence of the coefficient of thermal expansion (*CTE*) on the degree of crystallization of $CaMgSi_2O_6$ with Al_2O_3 specimens sintered at 900 °C for 3 h. The *CTE* of sintered specimens was increased with measurement temperature. With the addition of Al_2O_3 up to 8 vol.%, the *CTE* of the specimens was decreased due to the decrease of the degree of crystallization. As confirmed in Fig. 4, the rigidity of glass network was not changed remarkably for the specimens with

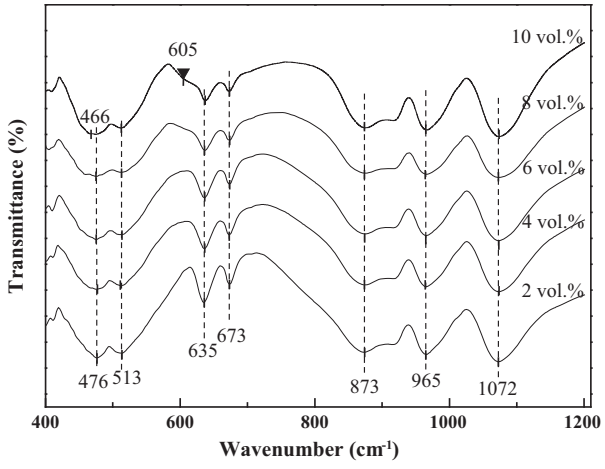

Fig. 4. FTIR spectra of $CaMgSi_2O_6$ with Al_2O_3 specimens sintered at 900 °C for 3 h.

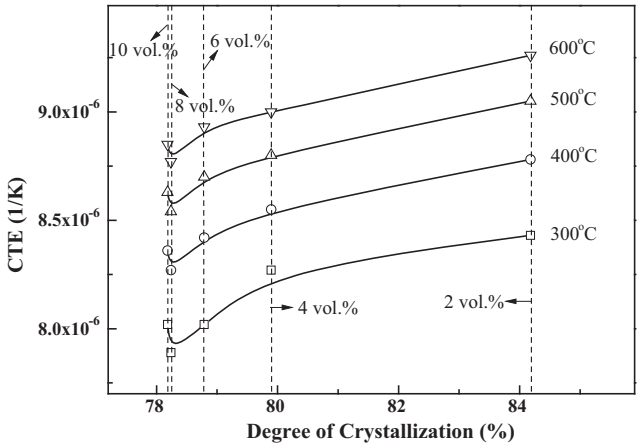

Fig. 5. Dependences of the coefficient of thermal expansion on the degree of crystallization of $CaMgSi_2O_6$ with Al_2O_3 specimens sintered at 900 °C for 3 h.

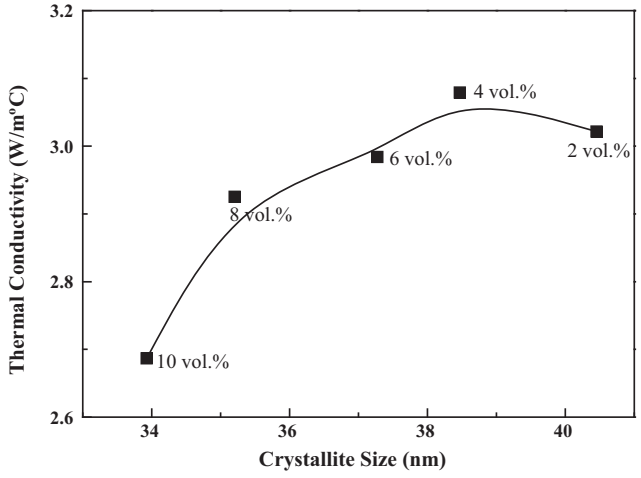

Fig. 6. Dependences of the thermal conductivity on the crystallite size of $CaMgSi_2O_6$ with Al_2O_3 specimens sintered at 900 °C for 3 h.

Al_2O_3 content up to 8 vol.%, however, that of the specimens with 10 vol.% of Al_2O_3 was decreased. Therefore, *CTE* of the sintered specimens with 10 vol.% of Al_2O_3 was increased.

The dependences of the thermal conductivity on the crystallite size of $CaMgSi_2O_6$ with Al_2O_3 specimens sintered at 900 °C for 3 h are shown in Fig. 6. With increasing of Al_2O_3 content, the thermal conductivity of the sintered specimens was increased up to 4 vol.% of Al_2O_3 due to the high thermal conductivity of Al_2O_3 (28–35 W/m °C) [3] and then decreased. For the specimens with higher content of Al_2O_3 than 4 vol.%, the decrease of thermal conductivity could be attributed to the increase of interface area resulted from the decrease of crystallite size, which are agreed with SEM micrographs (Fig. 3). Although the crystallite size of the specimens with lower content of Al_2O_3 than 4 vol.% was changed, the thermal conductivity was more affected by the thermal conductivity of Al_2O_3 than crystallite size.

4. Conclusions

Thermal properties of $CaMgSi_2O_6$ glass–ceramics with Al_2O_3 were investigated through the sintering temperature at 900 °C for 3 h after holding at 745 °C for 3 h. With the increase of Al_2O_3 content, the glass transition temperature (T_g), onset temperature of crystallization (T_c) and temperature of crystallization (T_p) of the specimens were shifted to high temperature.

The thermal conductivity of the sintered specimens was increased up to 4 vol.% of Al_2O_3 and then decreased due to the decrease of the density and average crystallite size of the specimens. However, the coefficient of thermal expansion (*CTE*) was decreased up to 8 vol.% of Al_2O_3 due to the decrease of the degree of crystallization. For the specimens with 10 vol.% of Al_2O_3, the *CTE* was increased due to the decrease of rigidity of the glass network.

Acknowledgements

This work was supported by the Human Resources Development of the Korea Institute of Energy Technology Evaluation and Planning (KETEP) grant funded by the Korea government Ministry of Knowledge Economy.

References

[1] J.H. Kim, S.J. Hwang, W.K. Sung, H.S. Kim, Thermal and dielectric properties of glass–ceramics sintered based on diopside and anorthite composition, J. Electroceram. 23 (2009) 209.
[2] P. Pisciella, M. Pelino, Thermal expansion investigation of iron rich glass-ceramic, J. Eur. Ceram. Soc. 28 (2008) 3021–3026.
[3] R. Barea, M. Belmonte, M.I. Osendi, P. Miranzo, Thermal conductivity of Al_2O_3/SiC platelet composites, J. Eur. Ceram. Soc. 23 (2003) 1773–1778.
[4] J.T. Oh, P. Hing, H.S. Fong, Effect of sintering temperature mismatch on the thermal diffusivity of cordierite-AlN composite, J. Mater. Process. Technol. 89–90 (1999) 497–500.
[5] A. Goel, E.R. Shaaban, F.C.L. Melo, M.J. Ribeiro, J.M.F. Ferreira, Non-isothermal crystallization kinetic studies on $MgO–Al_2O_3–SiO_2–TiO_2$ glass, J. Non-Cryst. Solids 45 (2007) 652–655.
[6] R. Hill, A. Calver, A. Stamboulis, N. Bubb, Real-time nucleation and crystallization studies of a fluorapatite glass–ceramics using small-angle neutron scattering and neutron diffraction, J. Am. Ceram. Soc. 90 (2007) 763–768.
[7] H.S. Kim, R.D. Rawlings, P.S. Rogers, Quantitative determination of crystalline and amorphous phases in glass–ceramics by X-ray diffraction analysis, Br. Ceram. Trans. J. 88 (1989) 21–25.
[8] E.D. Jeong, J.S. Bae, T.E. Hong, K.T. Lee, B.K. Ruy, T. Komatsu, H.G. Kim, Thermal properties and crystallization kinetics of tellurium oxide based glasses, J. Ceram. Process. Res. 8 (2007) 417–420.
[9] R. Chen, Y. Wang, Y. Hu, C. Liu, Modification on luminescent properties of $SrAl_2O_4$: Eu^{2+}, Dy^{3+} phosphor by Yb^{3+} ions doping, J. Lumin. 128 (2008) 1180–1184.
[10] K. Omori, Analysis of the infrared adsorption spectrum of diopside, Am. Mineral. 56 (1971) 1607–1616.
[11] D. Sarkar, D. Mohapatra, S. Ray, S. Bhattacharyya, S. Adak, N. Mitra, Synthesis and characterization of sol-gel derived ZrO_2 doped Al_2O_3 nanopowder, Ceram. Int. 33 (2007) 1275–1282.